On the stability of the Atlantic meridional overturning circulation

Matthias Hofmann[1] and Stefan Rahmstorf

Potsdam Institute for Climate Impact Research, P.O. Box 601203, 14412 Potsdam, Germany

Edited by Hans Joachim Schellnhuber, Potsdam Institute for Climate Impact Research, Potsdam, Germany, and approved September 28, 2009 (received for review August 12, 2009)

One of the most important large-scale ocean current systems for Earth's climate is the Atlantic meridional overturning circulation (AMOC). Here we review its stability properties and present new model simulations to study the AMOC's hysteresis response to freshwater perturbations. We employ seven different versions of an Ocean General Circulation Model by using a highly accurate tracer advection scheme, which minimizes the problem of numerical diffusion. We find that a characteristic freshwater hysteresis also exists in the predominantly wind-driven, low-diffusion limit of the AMOC. However, the shape of the hysteresis changes, indicating that a convective instability rather than the advective Stommel feedback plays a dominant role. We show that model errors in the mean climate can make the hysteresis disappear, and we investigate how model innovations over the past two decades, like new parameterizations and mixing schemes, affect the AMOC stability. Finally, we discuss evidence that current climate models systematically overestimate the stability of the AMOC.

climate change | ocean circulation | thermohaline circulation | tipping points | ocean modeling

The Atlantic meridional overturning circulation (AMOC) comprises a northward near-surface flow from the tip of South Africa via the Benguela Current, the Gulf Stream, and the North Atlantic (NA) Current right up into the Arctic Ocean. The water sinks in deep-water formation regions in the Nordic and Labrador Seas and returns to the south at depths of 2,000–3,000 m. The large heat transport of this current system [$\approx 10^{15}$W (1, 2)] has a major effect on northern hemisphere climate (3). Paleoclimatic evidence points to instabilities in this current system and demonstrates that large and abrupt shifts in Atlantic ocean circulation have repeatedly occurred (e.g., during the last Glacial) and were associated with large and abrupt changes in surface climate (4).

Global temperatures are projected to increase by up to 6.4 °C by the year 2100 (5), accompanied by a more vigorous hydrological cycle leading to a stronger net precipitation over the northern Atlantic and increased river inflow as well as meltwater influx from a shrinking Greenland Ice Sheet. Moreover, higher sea surface temperatures will further decrease the density of waters in the Nordic Seas, inhibiting deep-water formation. The expected climate change has raised concerns about the future fate of the AMOC, and the International Panel on Climate Change (IPCC) (5) concluded that there is an up to 10% probability that the AMOC "will undergo an abrupt transition during the course of the 21st century". The impacts of such a transition would likely be severe (6).

Research over the past decades, starting with Stommel's seminal 1961 paper (7), has found interesting stability properties of the AMOC, reviewed, e.g., in ref. 8. In brief, the AMOC, at least in models, has a bistable regime in its parameter space, where deep-water formation can be "on" (as in present climate) or "off", depending only on initial conditions. For increasing freshwater inflow to the Atlantic, this bistable regime passes a saddle-node bifurcation to a monostable regime where only the off state exists. For lesser freshwater inflow, there is another monostable regime where only the on state exists. This nonlinear behavior is explained by the positive salt-advection feedback first described by Stommel (7). High salinity in the northern Atlantic helps to drive deep-water formation there and thus the AMOC. But it is the flow itself that maintains high salinity there (in a region of net precipitation) by bringing salty subtropical waters northward.

In the past decades, the AMOC was considered primarily thermohaline driven, which requires a strong role of turbulent mixing to bring buoyancy (i.e., heat) downward to deeper ocean layers. With recent observational estimates pointing to rather low turbulent mixing rates in the real ocean (9, 10), the alternative concept of a primarily wind-driven AMOC has arisen (11, 12). These driving mechanisms have recently been reviewed by Kuhlbrodt et al. (2007) (13).

These findings have caused a reexamination of the AMOC stability properties, and some authors have argued on theoretical grounds that a predominantly wind-driven AMOC would not show the freshwater hysteresis found in the relatively diffusive ocean models (14–16), whereas others have argued that it would (17).

Progress in numerical techniques now allows us to test these hypotheses. It was shown in ref. 18 that the nearly nondiffusive second-order moments (SOM) tracer advection scheme of Prather (1986) (19) leads to an AMOC predominantly driven by the winds in a coarse-resolution ocean model in the limit of low vertical diffusion. Here we present freshwater hysteresis studies with such an ocean model. We present these results in the context of a broader discussion of the realism of AMOC stability in models and the changes that have been brought by advances in coarse-resolution ocean and climate modeling over the past decades.

Stability of Different Model Classes. Investigating the equilibria and stability properties of the ocean circulation requires the integration of models over very long time spans. It takes several thousand years for the ocean circulation to approach a thermodynamic equilibrium state because of the slow mixing time scale in the ocean. In equilibrium, properties like the interior temperature and salinity fields are determined by a balance between the diffusive and advective transport processes (the former representing turbulent mixing). Hence, modern models will take even longer to reach equilibrium than the generally more diffusive older models, and an integration time of 5,000 years or more may be required. To compute hysteresis curves as shown, e.g., in Figs. 1–3 requires many thousands of years of integration (the results shown in this paper overall required ≈8,000 years of model simulation).

Most investigations of the stability properties of the AMOC have been performed with models of intermediate complexity (EMICs), including ocean general circulation models (OGCMs) coupled to highly simplified atmospheres. This simplification raises the question of whether these EMICs have at least qualitatively the same

Author contributions: M.H. and S.R. designed research; M.H. performed research; and M.H. and S.R. wrote the paper.

The authors declare no conflict of interest.

This article is a PNAS Direct Submission.

[1]To whom correspondence should be addressed. E-mail: hofmann@pik-potsdam.de.

This article contains supporting information online at www.pnas.org/cgi/content/full/0909146106/DCSupplemental.

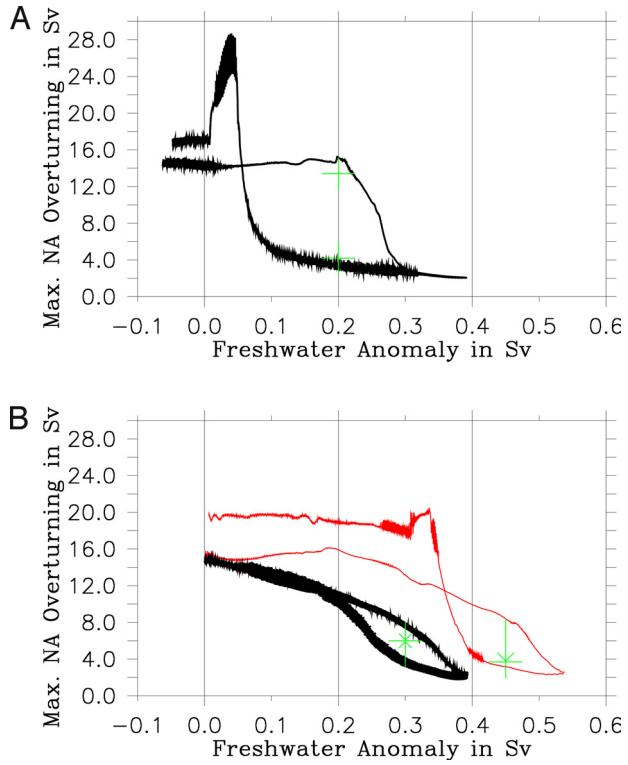

Fig. 1. Maximum strength of the AMOC in Sv against the freshwater anomaly supplied to the NA between 30° and 50 °N for experiments *STANDARD* (*A*) and *CLIMBER* (black line) and *BRIDGE* (red line) (*B*). (*A*) Experiment *STANDARD* reveals a hysteresis curve with a stable ''on'' state and ''off'' state. Equilibrium experiments using an anomalous freshwater forcing F_h of 0.2 Sv provide two distinct values for the maximum NA overturning strength: 13.8 Sv and 4.5 Sv (green crosses). (*B*) Experiments *CLIMBER* and *BRIDGE* reveal a very narrow hysteresis curve for F_h values >0.2 Sv. Equilibrium runs with both models at $F_h = 0.3$ Sv and $F_h = 0.45$ Sv (green arrows and crosses) show that the upper and lower branch of the hysteresis loop for *CLIMBER* and *BRIDGE* converge against each other.

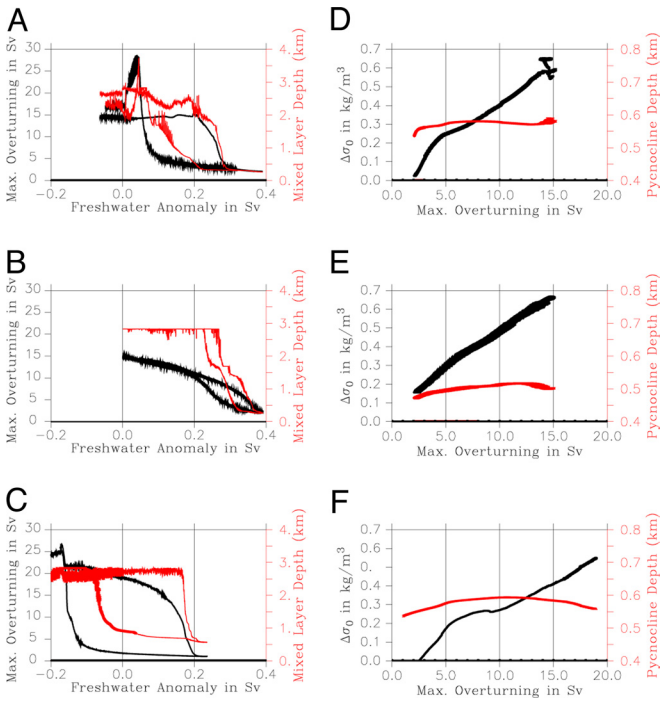

Fig. 3. Hysteresis curves for the maximum Atlantic overturning strength and NA mixed layer depths, meridional density gradients, and mean Atlantic pycnocline depth. (*A*) Maximum strength of Atlantic overturning (black) and maximum mixed layer depth in the Labrador and Nordic Seas between 60° and 80 °N (red) versus the anomalous freshwater flux over the NA for experiment *STANDARD*. (*B* and *C*) The same as in *A* but for *CLIMBER* and *HISTORIC-1*, respectively. (*D*) Zonal mean Atlantic potential density difference at depth of 750 m between 50 °N and 35 °S (black) and Atlantic mean pycnocline depth (red) (16) as a function of the maximum strength of the Atlantic overturning for experiment *STANDARD*. (*E* and *F*) The same as in *D* but for experiments *CLIMBER* and *HISTORIC-1*, respectively.

stability properties as atmosphere–ocean general circulation models (AOGCMs).

A spontaneous recovery of the AMOC from a shutdown after a freshwater pulse is an indication that a model is in the monostable regime, but it must not be misinterpreted as evidence for a lack of hysteresis: Many EMICS operate in a monostable regime for present climate, but still show hysteresis (8). Likewise, a linear response to freshwater perturbations on short (i.e., century) time scales (20) must not be misinterpreted as evidence for a lack of hysteresis and nonlinearity in the equilibrium response. The linear response on century time scales is fully reproduced, e.g., in the CLIMBER-2 model, which shows a well-documented hysteresis (21).

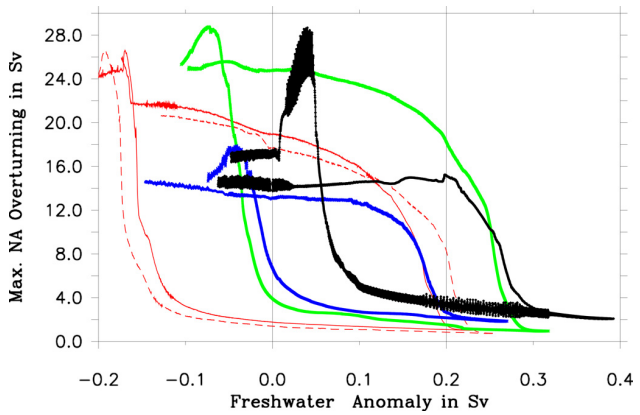

Fig. 2. Hysteresis curves for the *HISTORIC* model set compared with *STANDARD*. Full red line, *HISTORIC-1*;dashed red line, *HISTORIC-2*; green line, *HISTORIC-3*; blue line, *HISTORIC-4*; black line, *STANDARD*. For details see *Dependence on Parameterizations and Numerical Schemes*.

Comparing the response of AOGCMs and EMICs requires model comparisons where exactly the same experiments are performed with both model types. Two relevant intercomparison studies have been published. Stouffer et al. (22) found that "EMICs and AOGCMs obtain similar THC responses and climate changes". And Gregory et al. (23) found "no systematic differences in their simulations of THC behavior on decadal timescales". The IPCC report concluded that "the long-term stability of the AMOC found in the present AOGCM simulations is consistent with the results from the simpler models". At this stage, we conclude that despite many experiments no systematic differences between AOGCMs and EMICs in the stability properties of the AMOC have as yet been documented and that its hysteresis is a very robust property. This conclusion is corroborated further by the similarity in the response between different EMICs, which often show great differences in model design. However, final conclusions can only be drawn once full hysteresis experiments have been performed with AOGCMs.

Stability of a Predominantly Wind-Driven Conveyor. In this section, we investigate the hysteresis behavior of an ocean model employing

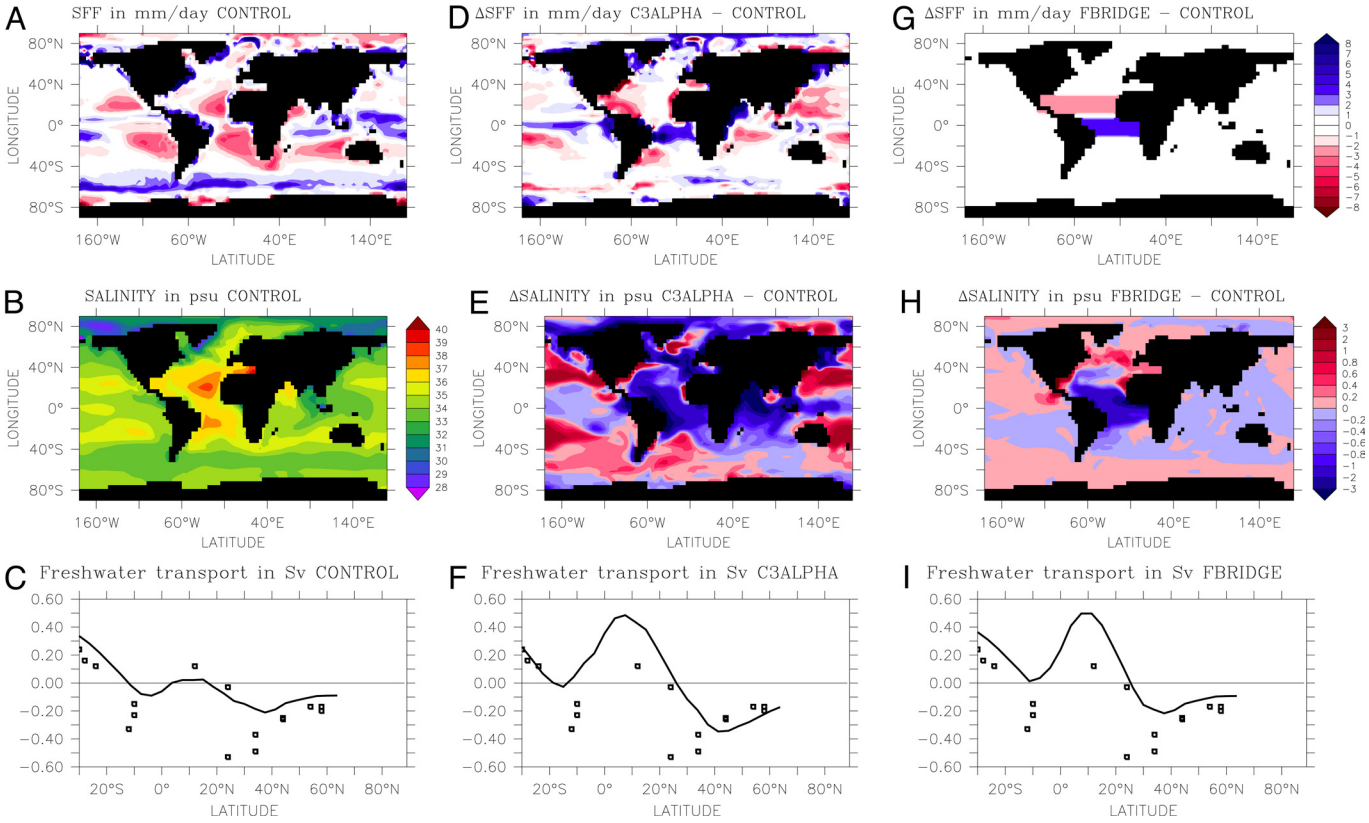

Fig. 4. Turbulent air–sea surface freshwater fluxes (SFF) (in Sv), sea surface salinity [(SSS), in practical salinity units (PSU)], and Atlantic MFT (in Sv) for the climatological mean state. (*A*) The SFF distribution provided by *STANDARD* reveals a characteristic spatial pattern with net precipitation in the tropics and mid–high latitudes and net evaporation over the subtropical gyres. (*B*) The simulated *STANDARD* SSSs resemble the observational data (47) (see Fig. S1*b*). (*C*) Comparison of the northward Atlantic MFT from *STANDARD* (black curve) with observational data (black squares) compiled by Wijffels (48). (*D* and *G*) Difference of the SFF between simulations *CLIMBER* and *STANDARD* and between *BRIDGE* and *STANDARD*, respectively. Note that the SFF distributions reveal a much higher net evaporation over the North Atlantic Subtropical Gyre and a higher net precipitation over Atlantic equatorial regions compared with *STANDARD*. (*E* and *H*) Difference of SSSs between simulations *CLIMBER* and *STANDARD* and between *BRIDGE* and *STANDARD*, respectively. (*F* and *I*) The same as in *C* but for *CLIMBER* and *BRIDGE*, respectively.

the SOM tracer advection scheme combined with realistically low vertical background diffusivities on the order of 0.1 cm^2s^{-1} (9, 10). It was already shown in ref. 18 that when employing the nearly nondiffusive SOM tracer advection scheme by Prather (19) in a coarse-resolution ocean general circulation model (OGCM) running in the limit of very low vertical diffusivities, about two thirds of the North Atlantic Deep Water resurfaces in the Southern Ocean, providing an AMOC predominantly driven by the winds. To the best of our knowledge, this was the first coarse-resolution OGCM simulation to reveal a global large-scale circulation pattern closely resembling that of the "reconfigured conveyor belt" by Toggweiler and Samuels (11, 12), in which the bulk of the global ocean upwelling occurs in the Southern Ocean. Besides forcing the upwelling in the Southern Ocean, the winds play an important role in driving the surface currents, notably in the transport of dense surface and subsurface water masses toward regions of deep-water formation and the Ekman suction of subsurface waters in the center of the subpolar gyres.

To be comparable with results of most of the previous studies on the AMOC hysteresis (24–27), we use the MOM3 OGCM coupled to a simple atmospheric energy balance model (MOM3-EBM). After integrating our standard model MOM3-EBM (see *Methods*) over more than 5,000 years, a quasisteady state was reached. During the last year of simulation, the turbulent sea surface freshwater fluxes (SFF_STANDARD) were written to a file for each integration time step. Subsequently, our standard model was spun-up for a further 500 years, driven by the diagnosed freshwater fluxes SFF_STANDARD, which defines the mean climatological starting point of the hysteresis experiment *STANDARD*. The details of the model configurations applied in the hysteresis experiments can be found in Table S1.

In steady state, the *STANDARD* configuration provides a maximum Atlantic overturning strength of ≈14.5 Sv (1 Sv = $10^6 m^3 s^{-1}$) with a maximum northbound meridional heat transport of ≈0.9 PW (1 PW = 10^{15}W). The turbulent freshwater fluxes at the sea surface calculated from precipitation minus evaporation plus river runoff (P−E+R) reveal a typical pattern with positive values (net precipitation) in the tropics and mid to high latitudes and negative values (net evaporation) in subtropical regions (see Fig. 4*A*). The simulated averaged air–sea freshwater flux over the Atlantic of −0.44 Sv between 40 °S and the equator and −0.14 Sv between the Equator and 40 °N is in line with values deduced from the freshwater fluxes of the Southampton Oceanography Centre database (28) combined with river runoff data from the Geophysical Fluid Dynamics Laboratory's corrected normal-year forcing dataset (available at http://data1.gfdl.noaa.gov:9192/opendap/CNYF_1p0/contents.html) (see Fig. S1*a*).

Starting from the climatological mean state, which is interpreted as the preindustrial climate, the NA was subjected to a steadily increasing freshwater flux between 30 °N and 50 °N at a slow rate of 0.1 Sv per 1,000 years, which allows to keep the model close to a steady state. This freshwater anomaly in the Atlantic Ocean was compensated by an inverse freshwater flux over the entire Pacific Ocean. Once the AMOC had shut down, the rate of the anomalous freshwater flux (F_h) was reversed.

The *STANDARD* model experiment entails a complete hyster-

esis of the AMOC, although the upper branch does not resemble a classical shape of a parabolic function as predicted from Stommels model (7, 25, 29). In Fig. 1*A*, the upper branch of the hysteresis, showing the maximum AMOC strength in the NA, appears to be independent of the freshwater anomaly up to a value of 0.2 Sv, whereas the overturning decreases rapidly when further increasing F_h by up to 0.3 Sv. Above this value, only an off state of the AMOC exists. While decreasing the anomalous freshwater flux, the overturning starts to recover when crossing a threshold value of ≈0.1 Sv, providing a typical freshwater hysteresis. The recovery of the AMOC is associated with a transient overshooting to large values because of a release of stored potential energy from the water column.

To test whether the hysteresis is only an artifact resulting from deviations from the steady state owing to F_h changing too rapidly, we have performed two additional equilibrium runs over more than 3,000 years. In both experiments, we have applied an anomalous freshwater flux of $F_h = 0.2$ Sv to the NA, which has been started from the upper and the lower hysteresis branch. As a result, at $F_h = 0.2$ Sv, the AMOC reveals two stable states (bistability), one with a maximum overturning strength of 14.3 Sv and an off state (Fig. 1*A*). These results confirm that the AMOC hysteresis is a robust result even if the model is run in a low-diffusion limit.

The upper branch of the AMOC hysteresis in the *STANDARD* experiment (Fig. 3*A*) deviates from a parabolic form, which is known as a characteristic feature when the salt-advection feedback plays the dominant role (25, 29). A comparison between the maximum NA overturning and the maximum mixed layer depth in the NA reveals a strong correlation between these two quantities (Fig. 3*A*). As long as the mixed layer depth remains in a range between 2,250 to 2,500 m, the maximum NA overturning is nearly constant at a value of ≈14 Sv. When increasing the freshwater anomaly beyond the threshold of 0.2 Sv, the mixed layer depth declines together with the overturning approaching the off state at $F_h = 0.3$ Sv. This decline suggests that in the *STANDARD* experiment the instability of deep-ocean convection (30), rather than the salt-advection feedback, determines the shape of the AMOC hysteresis. It should also be mentioned that the upwelling of relatively warm and salty subsurface waters (50–300 m) in the center of the cyclonic North Atlantic Polar and Subpolar Gyres helps to keep the convection in an on state (Fig. S2*a*).

Effect of Freshwater Climatology on AMOC Stability. Next, we investigate the impact of the spatial pattern of the freshwater forcing in the mean climatological state on the hysteresis. For this investigation, we use a second field of surface freshwater fluxes from an equilibrium run of the fully coupled Earth system model CLIMBER-3α (31). We refer to this second set as SFF_CLIMBER, (Fig. 4*D*) which, besides other differences, deviates from SFF_STANDARD by a higher net evaporation over the subtropical NA and greater net precipitation south of the Equator. Between 40 °S and the equator, the averaged freshwater flux into the Atlantic amounts to −0.06 Sv, whereas between the equator and 40 °N this value is −0.67 Sv, significantly deviating from the distribution pattern inferred from observational data (Fig. S1*a*). The northward Atlantic meridional freshwater transport (MFT) reveals a much stronger convergence and divergence between 10 °S and 10 °N and 10 °N and 40 °N, respectively, than in SFF_STANDARD (Fig. 4*F*). The second mean climatological state provided by the integration of MOM3-EBM, by using the new SFF_CLIMBER freshwater fluxes, defines the starting point of the hysteresis experiment *CLIMBER*.

To further test the effect of freshwater fluxes in the tropical Atlantic, a third type of freshwater fluxes was derived from SFF_STANDARD. Starting from SFF_STANDARD (Fig. 4*A*), subtracting an amount of 0.50 Sv over the NA in the latitudinal band between 15 °N and 30 °N and adding it between 7.5 °S, and 7.5 °N, resembling a "freshwater bridge", provides the turbulent freshwater fluxes SFF_BRIDGE (Fig. 4*G*), which impose a southward shift of the Intertropical Convergence Zone compared with SFF_STANDARD. Adopting SFF_BRIDGE in an equilibrium run of MOM3-EBM provides the mean climatological state for experiment *BRIDGE*. Fig. 4*I* shows the northward Atlantic MFT, which mostly resembles that of SFF_CLIMBER (Fig. 4*F*).

Both models have been subjected to a slowly changing F_h identical to that of the experiment *STANDARD*. As depicted in Fig. 1*B*, the experiments start with a similar maximum AMOC strength that continuously declines when F_h increases, neither resembling a classical shape of a Stommel-like parabolic function nor a shape comparable with the *STANDARD* experiment (Fig. 1*B*). The two branches only describe a very narrow loop at F_h values larger than 0.2 Sv and 0.35 Sv for *CLIMBER* and *BRIDGE*, respectively. The existence of two stable states at F_h values lower than 0.35 Sv for experiment *BRIDGE* can be explained by the bistability of Labrador Sea convection.

Additional equilibrium runs of *CLIMBER* and *BRIDGE* at $F_h = 0.3$ Sv and $F_h = 0.45$ Sv, respectively, show that the two narrow hysteresis branches converge to each other after an equilibration time of more than 3,000 years (Fig. 1*B*). As a result, a robust freshwater hysteresis does not exist. The narrow hysteresis loops must be regarded as an artifact arising from the models inertia, i.e., the model not always stays close enough to the steady state.

Experiment *CLIMBER* starts with a present-day NA salinity distribution that is fresher than that of *STANDARD* (see Fig. 4*E* and Fig. S2*c*) although the overturning strengths are comparable. As the NA freshwater anomaly increases up to the value of $F_h = 0.25$ Sv, the maximum overturning strength declines from 15 Sv to 10 Sv. Beyond this value, the convection in the NA ceases (Fig. 3*B*), whereas at $F_h = 0.39$ Sv the off state is reached.

Experiment *BRIDGE* shows that the crucial difference between *CLIMBER* and *STANDARD* is the (unrealistic) relocation of tropical rainfall from the northern to the southern tropical Atlantic in the former. In this case, the salty water required to maintain deep-water formation in the North does not need to be advected across the equator from the southern hemisphere. Rather, it derives from the Northern Subtropics, from which it can be brought north effectively by the wind-driven surface currents, i.e., the Subtropical and Subpolar Gyre circulations. The role of the large-scale AMOC in maintaining relatively high salinities in the northern Atlantic is thus diminished; Stommel's salt advection feedback is therefore disabled, and the cause of the hysteresis response vanishes. This view is supported by the fact that the cross-equatorial freshwater transport has the opposite sign in *STANDARD* (Fig. 4*C*) versus *BRIDGE* (Fig. 4*F*) and *CLIMBER* (Fig. 4*I*). In the latter two, the cross-equatorial freshwater transport is strongly positive, i.e., the ocean circulation makes the NA fresher, not saltier. Already, Rahmstorf (29) argued that the hysteresis of the AMOC is not due to a localized salt advection from the northern subtropics, but rather is due to a large-scale salt transport from the southern to the northern hemisphere, as witnessed by the fact that the entire NA north of the equator gets fresher when the AMOC is shut down in models showing the classical hysteresis.

Dependence on Parameterizations and Numerical Schemes. In this section, we investigate how the stability properties of the AMOC in climate models have changed as the ocean models have become more sophisticated over recent decades. For that purpose, we have set up a series of four additional models derived from the *STANDARD* configuration by changing physical and numerical aspects. Because all of the following experiments use the SFF_STANDARD freshwater fluxes, the climatological difference at the sea surface remains negligibly small. We refer to these four model setups as *HISTORIC* followed by the numbers 1 to 4.

HISTORIC-1. In the first approach, we have tried to get as close as possible to a model configuration used by Rahmstorf (24, 25, 29).

Therefore, we use the simple central in time, central in space (CTCS) tracer advection scheme instead of SOM (see *Methods*). The standard parameterization of vertical diffusion with a very low background value (0.1 cm^2s^{-2}), which also accounts for bottom-enhanced vertical mixing was replaced by a Bryan–Lewis type diffusivity (32) with values varying between 0.3 cm^2s^{-2} in the upper ocean and 1.3 cm^2s^{-2} in the abyss. The Gent–McWilliams parameterization of mesoscale eddies (33) was removed and isopycnal mixing (34) replaced by a horizontal diffusion that varies with depth, with values changing between 1.0×10^7 cm^2s^{-2} at sea surface and 0.5×10^7 cm^2s^{-2} at the bottom.

The resulting hysteresis graph for experiment *HISTORIC-1* is shown in Fig. 2 (full red line). The hysteresis reveals a typical shape with a parabolic upper branch resembling those shown in earlier studies (25, 29). In the present-day state the AMOC is bistable and the bifurcation point is approximately located at $F_h = 0.15$ Sv. The width and height of the *HISTORIC-1* hysteresis loop is about twice as wide as the *STANDARD* hysteresis. The overturning ceases before the convection in the NA is shut down, leading to a parabolic, Stommel-like hysteresis (Fig. 3*C*).

HISTORIC-2. The second model configuration deviates from *HISTORIC-1* only in the changing of the parameterization of vertical diffusion to the *STANDARD* model. Surprisingly, the resulting hysteresis (Fig. 2, red dashed line) is nearly identical to the hysteresis of experiment *HISTORIC-1*, revealing that the impact of a lowering of the vertical background diffusivities from 0.3–1.3 to 0.1 cm^2s^{-1} on the sensitivity of the AMOC is minor or possibly masked by numerical diffusion.

HISTORIC-3. The third configuration, is the same as the previous *HISTORIC-2* but with the SOM tracer advection scheme instead of CTCS. This experiment demonstrates that the replacement of the CTCS advection scheme by the much more elaborated SOM scheme has a big impact on the location and shape of the AMOC hysteresis (Fig. 2, green line). In comparison with the previous *HISTORIC-2*, the *HISTORIC-3* hysteresis is shifted toward higher freshwater fluxes by a concomitant contraction along the freshwater anomaly axis and a stretching along the overturning axis while keeping the parabolic shape of the upper branch.

HISTORIC-4. Adding the Gent–McWilliams (33) parameterization of mesoscale eddy fluxes to *HISTORIC-2* and replacing horizontal mixing by isopycnal diffusion results in the fourth model configuration, *HISTORIC-4*. The comparison between *HISTORIC-4* and *HISTORIC-2* allows us to infer the impact of the parameterization of mesoscale eddies on the AMOC hysteresis. Accounting for the effects of mesoscale eddies leads to a shift of the hysteresis toward higher F_h values and a narrowing of its width (Fig. 2, blue line). When replacing the CTCS advection scheme used in *HISTORIC-4* by SOM, we are back to the hysteresis of the *STANDARD* configuration (Fig. 2, black line).

Bottom Line of the Results. In our simulations, we found that once deep convection and, thus, deep-water formation in the NA is prohibited by the existence of a freshwater lid, the northbound water masses from the Southern Ocean cannot penetrate far enough into the Atlantic basin. They sink between 40 °S and 30 °S where they return southward at greater depth and move toward the Antarctic Divergence Zone (see Fig. S3). Hence, this reduced southern hemispheric overturning cell can be regarded as a short circuit of the AMOC, which has been already discussed in ref. 35.

These results confirm that the existence of a hysteresis is a robust property across a number of changes to model parameterizations. However, the exact shape and size of the hysteresis and, equally important, the position of present-day climate on the hysteresis loop, does depend on model details, raising the question of how realistic current models are in this respect.

Do Current Models Have Realistic Stability Properties? Substantial research effort has been devoted to understanding the stability properties of the AMOC in models, but surprisingly little work has been devoted to finding ways to link the models' stability properties to those of the real ocean.

Anecdotal evidence suggests that many modeling groups (including our own) have encountered problems with an unstable AMOC, to the extent that it collapsed in their present-day model climate. These problems are seen as a model deficiency that in most cases would not be published but repaired by changes to the model, e.g., those that affect the Atlantic's surface freshwater budget. A highly stable AMOC, on the other hand, would give good results for present-day climate and hence be retained. Arguably, this selection process during model development could have biased our current suite of models toward greater stability.

Unfortunately, the stability of the real present-day AMOC is not easily determined. However, a series of studies (27, 29, 36, 37) concluded that the freshwater transport by the AMOC could serve as a stability indicator: If the AMOC exports freshwater from the Atlantic basin, the Atlantic would become fresher after an AMOC shutdown. This freshwater accumulation near the surface would prevent a recovery of the AMOC and lead to a stable off state. Hence, an AMOC that exports freshwater should be in the bistable regime, one that imports freshwater should be in the monostable regime.

This idea has since been pursued and confirmed in several studies. Based on observational data, Weijer (38) found that the real AMOC exports freshwater from the Atlantic across 30 ° S (at a rate of ≈0.3 Sv); this indicates it may be bistable. An analysis of nine climate models in contrast found that all but one import freshwater via the AMOC (Weber et al. in ref. 39). For one of these models, it has been diagnosed that the AMOC exports freshwater (≈0.1 Sv) in the first decades after model initialization with observed data, when the temperature and salinity fields are still close to those of the real ocean and the model has established a flow pattern consistent with these fields (40). Later on, the model drifts to a state where "large salinity errors" develop, the AMOC imports freshwater (≈0.3 Sv), and, presumably, the AMOC has switched from bistable to monostable.

Thus, there is evidence suggesting that our current generation of models may have qualitatively incorrect stability properties, with their AMOC in the monostable regime whereas the real ocean may be in the bistable regime. Note that this implies that the models may be far too stable with respect to perturbations like those resulting from global warming due to increased river discharge and Greenland meltwater influx (41, 42) because the monostable regime is far away from the bifurcation point where an AMOC collapse is initiated.

Conclusion

We have investigated the stability properties of the AMOC in a series of dedicated model experiments with a model of intermediate complexity as well as a review of a number of model studies by other authors. Our first conclusion is that hysteresis behavior of the AMOC with respect to freshwater input at the sea surface is a highly robust phenomenon that is also found in a model running in the limit of low mixing, resembling the predominantly wind-driven conveyor proposed by Toggweiler and Samuels (11, 12). This finding supports a theoretical result of Fürst (17). Given that so far no major differences have been found in the AMOC response of different model classes, we expect this result to carry over also to state-of-the-art coupled climate models.

We find that the hysteresis response of the AMOC can be suppressed but only by a major change in the surface freshwater balance that disables Stommel's salt advection feedback and thus removes the underlying cause of the hysteresis behavior. We also find that a series of model improvements that have become

commonplace in recent years, like new mixing and advection schemes, do not fundamentally alter the hysteresis behavior, although they do affect the details of the hysteresis loop and the position of present-day climate on it. The AMOC thus remains a classical "tipping point" (43) in the sense that it has a well-defined threshold with respect to freshwater as an external control parameter.

But how realistic is the position of present-day climate on the stability diagram and thus its proximity to the critical Stommel threshold? This is a crucial question because it determines the amount of additional freshwater added to the NA that would initiate a shutdown of the AMOC, a question highly relevant for its response to future global warming. This issue remains unresolved. However, substantial evidence suggests that current models may be systematically too stable in that they are in a monostable regime far away from the threshold, in contrast to what observational data suggest. This possibly excessive stability is exacerbated by the fact that most current climate models [including all in the general circulation model ensemble discussed in the 2007 IPCC report (5)] do not account for the growing freshwater runoff from a melting Greenland ice sheet. A recent counterexample is Hu et al. (2009) (42). As a ball-park number, melting all Greenland ice in 1,000 years corresponds to an average freshwater influx of 0.1 Sv. These model deficiencies make a risk assessment for AMOC changes very difficult at present and require urgent research attention.

Methods

The model used in this study consists of an improved version of the OGCM MOM-3 (31), coupled to a state-of-the-art dynamic/thermodynamic sea-ice model (44) and a simple anomaly model of the atmospheric energy–moisture balance (18), which allows us to approximately account for the stabilizing temperature feedback. In the following, we refer to this model as MOM3-EBM. In this approach, the atmospheric forcing is provided by climatological data. We do not apply a relaxation term toward observed sea surface temperature and salinity data. This method allows for a more realistic representation of the turbulent air–sea fluxes than coupling an intermediated complexity atmospheric model. This study uses the National Centers for Environmental Predictions/National Center for Atmospheric Research reanalysis data (45).

The horizontal resolutions of the atmospheric model and the ocean–sea ice model are identical when using a uniform grid mesh size of $3.75° \times 3.75°$. In the vertical, the grid consists of 24 levels with thickness increasing from 25 m at top to 500 m at the bottom. The model incorporates a nonlinear free surface and includes an empirical parameterization of bottom-enhanced vertical mixing described in ref. 46 with a low background diffusivity of 0.1 $cm^2 s^{-1}$. Isopycnal Redi stirring (34) is set to 1.0×10^7 $cm^2 s^{-1}$, whereas the constant Gent–McWilliams thickness diffusivity (33) is $0.25 \times 10^7 cm^2 s^{-1}$. The OGCM benefits from a SOM tracer advection scheme (19), which is nearly free of spurious diffusion and dispersion. The SOM advection scheme allows for simulating a more realistic distribution of oceanic tracers, notably of frontal systems (18).

ACKNOWLEDGMENTS. This work was supported by German Science Foundation Grant RA977/5–1.

1. Bryden HL, Imawaki S (2001) Ocean heat transport. In *Ocean Circulation and Climate* (Academic, London) pp 455–474.
2. Ganachaud A, Wunsch C (2003) Large scale ocean heat and freshwater transports during the world ocean circulation experiment. *J Clim* 16:696–705.
3. Broecker WS (1991) The grat ocean conveyor. *Oceanography* 4:200–206.
4. Rahmstorf S (2002) Ocean circulation and climate during the past 120,000 years. *Nature* 419:207–214.
5. International Panel on Climate Change (2007) *The Physical Science Basis. Contribution of Working Group I to the Fourth Assessment Report of the Intergovernmental Panel on Climate Change* (Cambridge Univ Press, Cambridge, UK).
6. Kuhlbrodt T, et al. (2009) An integrated assessment of changes in the thermohaline circulation. *Clim Change* 96:489–537.
7. Stommel H (1961) Thermohaline convection with two stable regimes of flow. *Tellus* 13:224–230.
8. Rahmstorf S, et al. (2005) Thermohaline circulation hysteresis. *Geophys Res Lett*, 10.1029/2005GL023655.
9. Ledwell JR, Watson AJ, Law CS (1993) Evidence for slow mixing across the pycnocline from an openocean tracerrelease experiment. *Nature* 364:701–703.
10. Gregg MC, Sanford TB, Winkel DP (2003) Reduced mixing from the breaking of internal waves in equatorial waters. *Nature* 422:513–515.
11. Toggweiler JR, Samuels B (1993) *Is the Magnitude of the Deep Outflow from the Atlantic Ocean Actually Governed by Southern Hemisphere Winds*? NATO ASI Series, ed Heimann M (Springer, Berlin), pp 333–366.
12. Toggweiler JR, Samuels B (1993) *New Radiocarbon Constraints on the Upwelling of Abyssal Water to the Ocean's Surface*. NATO ASI Series, ed Heimann M (Springer, Berlin), pp 303–331.
13. Kuhlbrodt T, et al. (2007) On the driving processes of the atlantic meridional overturning circulation, doi:10.1029/2004RG000166.
14. Nof D, VanGorder S, Boer AMD (2007) Does the atlantic meridional overturning cell really have more than one stable steady state? *Deep Sea Res I* 54:2005–2021.
15. Keeling RF (2002) On the freshwater forcing of the thermohaline circulation in the limit of low diapycnal mixing. *J Geophys Res*, 107:10.1029/2000JC000685.
16. Gnanadesikan A, Toggweiler RJ (1999) Constraints by silicon cycling on vertical exchange in general circulation models. *Geophys Res Lett* 26:1865–1868.
17. Fürst J (2009) Conceptual model of oceanic overturning. Diploma thesis. (Potsdam Institute for Climate Impact Research, Potsdam, Germany).
18. Hofmann M, Maqueda MAM (2006) Performance of a second-order moments advection scheme in an ocean general circulation model. *J Geophys Res*, 10.1029/2005JC003279.
19. Prather MJ (1986) Numerical advection by conservation of second-order moments. *J Geophys Res* 91:6671–6681.
20. Rind D, deMenocal P, Russell G, Sheth S, Collins D (2001) Effects of glacial meltwater in the GISS coupled atmosphere ocean model: 1. North Atlantic Deep Water response. *J Geophys Res* 106:27335–27353.
21. Ganopolski A, Rahmstorf S (2001) Simulation of rapid glacial climate changes in a coupled climate model. *Nature* 409:153–158.
22. Stouffer R, et al. (2006) Investigating the causes of the response of the thermohaline circulation to past and future climate changes. *J Clim* 19:1365–1387.
23. Gregory J, et al. (2005) A model intercomparison of changes in the atlantic thermohaline circulation in response to increasing atmospheric co2 concentration. *Geophys Res Lett*, 10.1029/2005GL023209.
24. Rahmstorf S (1994) Rapid climate transitions in a coupled ocean-atmosphere model. *Nature* 372:82–85.
25. Rahmstorf S (1995) Bifurcations of the Atlantic thermohaline circulation in response to changes in the hydrological cycle. *Nature* 378:145–149.
26. Prange M, Lohmann G, Paul A (2003) Influence of vertical mixing on the thermohaline hysteresis: Analyses of an ogcm. *J Phys Oceanogr* 33:1707–1721.
27. Dijkstra HA (2007) Characterization of the multiple equilibria regime in a global ocean model. *Tellus* 59A:695–705.
28. Josy SA, Kent EC, Taylor PK (1998) *The Southampton Oceanography Centre (SOC) Ocean-Atmosphere Heat Momentum and Freshwater Flux Atlas*, Technical Report 6. (Southampton Oceanography Center, Southampton, UK).
29. Rahmstorf S (1996) On the freshwaterforcing and transport of the Atlantic thermohaline circulation. *Clim Dyn* 12:799–811.
30. Rahmstorf S (2000) The thermohaline ocean circulation—A system with dangerous threshoulds? *Climatic Change* 52:26–35.
31. Montoya M, et al. (2005) The earth system model of intermediate complexity CLIMBER-3α. Part I: Description and performance for present day conditions. *Clim Dyn* 25:237–263.
32. Bryan K, Lewis L (1979) A water mass model of the world ocean. *J Geophys Res* 84:2503–2517.
33. Gent PR, McWilliams JC (1990) Isopycnal mixing in ocean circulation models. *J Phys Oceanogr* 20:150–155.
34. Redi MH (1982) Oceanic isopycnal mixing by coordinate rotation. *J Phys Oceanogr* 12:1154–1158.
35. Toggweiler JR, Samuels B (1995) Effect of Drake Passage on the global thermohaline circulation. *Deep Sea Res I* 42:477–500.
36. DeVries P, Weber SL (2005) The atlantic freshwater budget as a diagnostic for the existence of a stable shut down of the meridional overturning circulation. *Geophys Res Lett*, 10.1029/2004GL021450.
37. Weber SL, Drijfhout SS (2007) Stability of the atlantic meridional overturning circulation in the last glacial maximum climate. *Geophys Res Lett*, 10.1029/2007GL031437.
38. Weijer W, de Ruijter WPM, Dijkstra HA, van Leeuwen PJ (1999) Impact of interbasin exchange on the Atlantic overturning circulation. *J Phys Oceanogr* 29:2266–2284.
39. Weber SL, et al. (2007) The modern and glacial overturning circulation in the Atlantic ocean in PMIP coupled model simulations. *Clim Past* 3:51–64.
40. Pardaens AK, Banks HT, Gregory JM (2003) Freshwater transport in hadCM3. *Clim Dyn* 21:177–195.
41. Jungclaus JH, Haak H, Esch M, Roeckner E, Marotzke J (2006) Will greenland melting halt the thermohaline circulation? *Geophys Res Lett*, 10.1029/2006GL026815.
42. Hu A, Meehl GA, Han W, Yin J (2009) Transient response of the moc and climate to potential melting of the Greenland Ice Sheet in the 21st century. *Geophys Res Lett*, 10.1029/2009GL037998.
43. Lenton TM, et al. (2008) Tipping elements in the Earth's climate system. *Proc Natl Acad Sci USA* 105:1786–1793.
44. Fichefet T, Maqueda MAM (1997) Sensitivity of a global sea ice model to the treatment of ice thermodynamics. *J Geophys Res* 102:12609–12646.
45. Kalnay E, et al. (1996) The NCEP/NCAR 40-years reanalysis project. *Bull Amer Meteorol Soc* 77:437–471.
46. Hasumi H, Suginohara N (1999) Effects of locally enhanced vertical diffusivity over rough bathymetry on the world ocean circulation. *J Geophys Res* 104:23367–23374.
47. Conkright M, Levitus S, Boyer T (1994) *World Ocean Atlas 1994 Volume 1*: *Nutrients* (U.S. Dept of Commerce, Washington, D.C.).
48. Wijffels SE (2001) Ocean transport of fresh water. In *Ocean Circulation and Climate* (Academic, London), pp 475–488.